Int. J. Microgravity Sci. Appl., **35** (2) (2018) 350203
DOI: 10.15011//jasma.35.350203

IIII Original Paper IIII

Analysis of Local Flame-Spread Characteristics of an Unevenly Arranged Droplet Cloud in Microgravity

Yasuko YOSHIDA[1], Narita SANO[1], Takehiko SEO[1], Masato MIKAMI[1], Osamu MORIUE[2], Yuji KAN[3] and Masao KIKUCHI[3]

Abstract

As a preliminary experiment of the "Group Combustion" experiment conducted in the Japanese Experiment Module "Kibo" aboard the International Space Station (ISS) in 2017, a combustion experiment of an unevenly arranged droplet cloud with 148 *n*-decane droplets tethered on a SiC-fiber lattice was conducted in microgravity during parabolic flight of an aircraft. In this study, three methods of identifying the local flame-spread direction were proposed to determine the local flame-spread rate between two adjacent droplets of an unevenly arranged droplet cloud considering the local flame-spread direction. The first method employed the vertical direction from the isothermal line to the unburned droplet. The isothermal line was approximated based on the luminance of SiC fibers tethering droplets. The second method considered the luminance distribution of the initial flame immediately after ignition. The third method compared the local flame-spread-rate candidates from neighboring droplets with the flame spread-rate of the linear droplet array. It was possible to identify the local flame-spread direction by any one of these methods, and the local flame-spread rate is calculated between two droplets close to this direction. The results suggest that there are many conditions under which the local flame-spread rate of an unevenly arranged droplet cloud is greater than the flame spread rate of the linear droplet array.

Keyword(s): Microgravity, Combustion experiment, Droplet cloud, Flame spread
Received 1 March 2018, Accepted 12 April 2018, Published 30 April 2018.

1. Introduction

Spray combustion, a liquid fuel combustion method widely used in practical combustors, is a complicated phenomenon in which physical and chemical processes proceed simultaneously. Its mechanism has not been revealed in detail. In continuous spray combustion seen in gas turbine engines, the flame spread in the spray occurs near the flame base. On the downstream side, most droplets of the spray are surrounded by a collective flame and group combustion occurs. The flame spread of the spray is also seen immediately after ignition in a diesel engine and plays an important role in the stable operation of combustors. Many researchers have studied the flame spread of droplet arrays in microgravity theoretically and experimentally as a fundamental research[1),2)]. As for group combustion, studies based on the steady-state theory have been conducted by Chiu et al [3)]. However, the relation between the flame spread and the group combustion, and the group combustion excitation mechanism have not been elucidated.

As an attempt to utilize the research results on the flame spread of a few droplets in microgravity to elucidate the group combustion excitation mechanism, Mikami et al. [4)] developed a percolation model describing the flame spread of randomly-distributed droplet clouds near the group-combustion-excitation limit. In addition, droplet-cloud-combustion experiments entitled "Elucidation of Flame Spread and Group Combustion Excitation Mechanism of Randomly Distributed Droplet Clouds (abbreviation: Group Combustion)" [5)] were conducted for the first combustion experiment in the Japanese experiment module "KIBO" aboard the international space station (ISS) in 2017. The purpose of the Group Combustion experiments was to investigate the effects of droplet interaction, free droplet and radiant heat loss on the flame spread between droplets using randomly-distributed droplet clouds with more than 100 droplets and droplet-cloud elements with a few droplets. As a preliminary experiment prior to the Group Combustion experiments aboard ISS, flame-spread experiments of droplet clouds were conducted in microgravity during parabolic flight of an aircraft to check the functions of the experimental apparatus Group Combustion Experiment Module (GCEM) and to establish the analysis method of the flame-spread characteristics for droplet clouds with many droplets.

The purpose of this study was to establish the analysis method of the local flame-spread characteristics of an unevenly arranged droplet cloud based on the parabolic flight experiments conducted as a preliminary experiment of the Group Combustion experiments. The local flame-spread direction was identified through a few methods and the local flame-spread rate between two adjacent droplets was obtained based on the results.

1 Yamaguchi University, 2-16-1 Tokiwadai, Ube, Yamaguchi 755-8611, Japan.
2 Kyusyu University, 744 Motooka, Nishi, Fukuoka 819-0385, Japan.
3 Japan Aerospace Exploration Agency, 2-1-1 Sengen Tsukuba, Ibaraki 305-8505, Japan.
(E-mail: w502wd@yamaguchi-u.ac.jp)

2. Experimental conditions and method

This research used the experimental device Group Combustion Experiment Module (GCEM)[6] shown in **Fig. 1** and conducted a flame-spread experiment of a droplet cloud in microgravity during parabolic flight operated by the Diamond Air Service. The droplet-cloud generation device and ignition device were installed in an aluminum combustion vessel with a volume of 14.3 L. The flame spread was observed from outside the combustion chamber by a digital video camera through a window made of sapphire glass. **Figure 2** shows the droplet support unit with a SiC-fiber lattice and the ignition unit. The droplets were generated one by one to form a droplet cloud at the designated intersection of a 30×30 lattice with 14-μm SiC fibers (Nihon Carbon, Hi-Nicalon) stretched at 4-mm intervals. The fuel was *n*-decane. A predetermined amount of fuel was pushed out from a syringe unit driven by a stepping motor through a Teflon tube, and the droplet was generated by supplying the fuel to an intersection of SiC fibers through a glass-tube needle whose tip was narrowed to an outer diameter of about 70 μm. The unevenly arranged droplet cloud was generated by repeating the droplet generation procedure while the position of the glass-tube needle was moved using a three-dimensional traverse device. A droplet near the center of one side of the SiC-fiber lattice was ignited by electrical heating of a Ni-Cr wire. As described by Mikami et al.[7] and Farouk and Dryer [8], the effect of a 14-μm SiC fiber on droplet combustion of 1 mm was negligible.

As shown in **Fig. 3**, 148 droplets were generated. The original purpose of this preliminary experiment was to check the functions of the apparatus and to determine whether the pressure inside the chamber during the flame-spread over so many droplets was lower than the permissible pressure of the combustion vessel. Therefore, the minimum droplet spacing was set to 8 mm so that the flame could spread to all the droplets. Since there were lattice points without droplets, it was a non-uniform droplet cloud. This study established the analysis method of the local flame-spread characteristics of an unevenly arranged droplet cloud. The flame spread of the droplet cloud was started by igniting Droplet 142 in **Fig. 3** with an ignition unit.

Figure 4 shows the initial droplet diameter just before the ignition in microgravity. The *y*-direction is a vertical direction from the lower side of **Fig. 3**, where the droplets are numbered in the generation order. Since the droplets were generated in normal gravity from the largest number position in the *y*- direction, the earlier generated droplet evaporated more until the ignition and the diameter decreased greatly. This study investigated the analysis method of the local flame-spread direction and the local flame-spread rate based on this droplet cloud. Although pre-vaporization occurred, the local equivalence ratio at the *n*-decane droplet surface was about 0.1 at room-temperature, which is much smaller than the lower flammability limit. Nomura et al. [9] conducted microgravity experiments of the flame spread of *n*-decane droplet arrays in fuel vapor/air mixtures and showed that such a small equivalence ratio does not affect the flame spread. In the Group Combustion experiments aboard ISS, the droplets were generated in consideration of pre-evaporation from the start

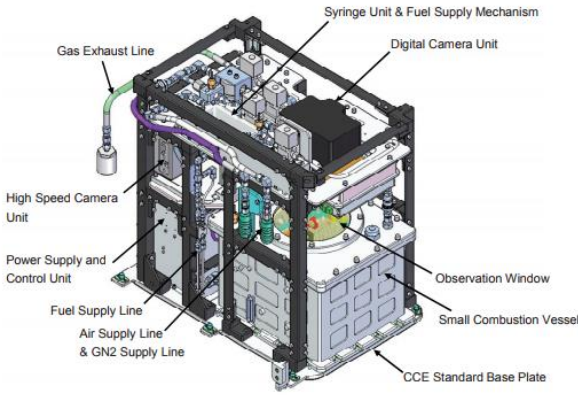

Fig. 1 Schematic of Group Combustion Experiment Module (GCEM) [6].

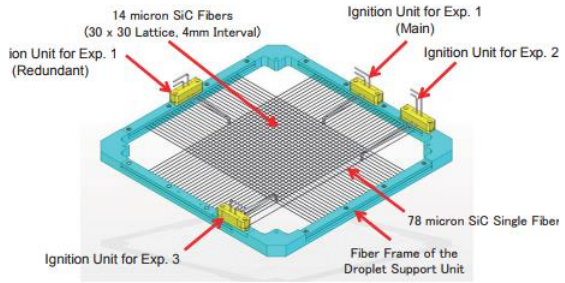

Fig. 2 Schematic of the droplet support unit and ignition unit [6].

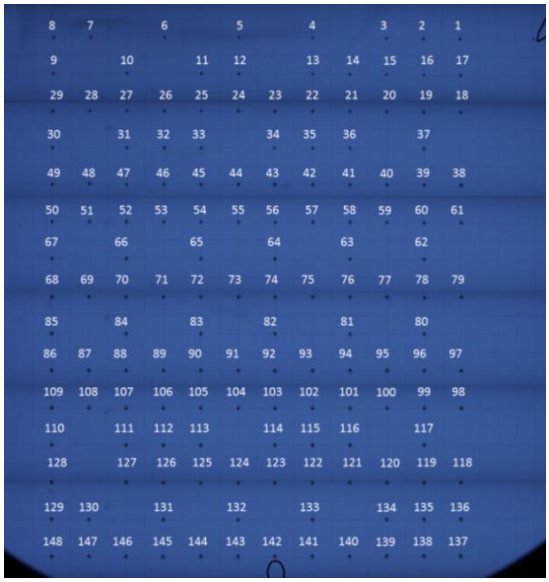

Fig. 3 Droplet arrangement on SiC-fiber lattice and droplet identification numbers.

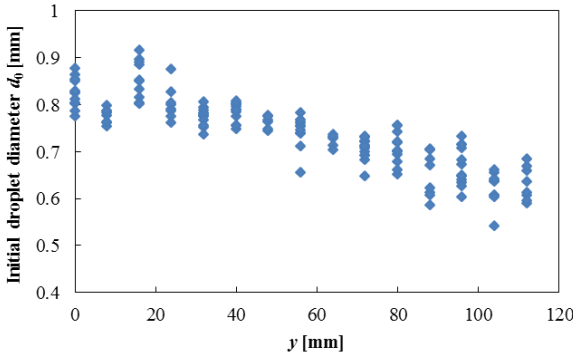

Fig. 4 The initial droplet diameter for different y-direction positions.

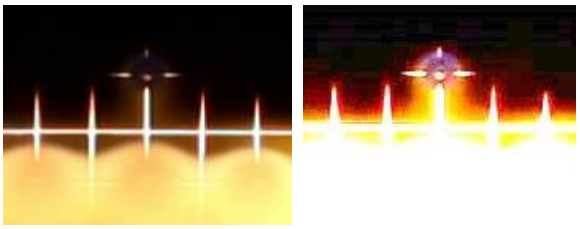

(a) Original image (b) Brightness maximized image

Fig. 5 Ignition identification method.

of droplet generation until the ignition, so that the droplet diameter was uniform at ignition. Just before the ignition, back-lit still images of the droplet cloud were taken using a digital video camera (Canon, EOS 5D Mark II), and the initial droplet diameter of each droplet was measured from the image. The number of pixels of a still image was 5616×3744 pixels, and the resolution was 41.5 μm/pixel. The flame spread behavior was photographed by the same digital video camera as that used for a movie. The number of pixels of the movie was 1920×1080 pixels, and the resolution was 122 μm/pixel. The frame rate was 30 fps, the exposure time was 1/60 s, and the ISO sensitivity was 1250.

The ignition timings of all droplets for each frame of the flame-spread movie were analyzed by image analysis. The ignition of a droplet was defined as the timing of the first appearance of the blue flame. Although the blue flame was not clearly confirmed in the original image as shown in **Fig. 5(a)**, the brightness maximized image shown in **Fig. 5(b)** clearly shows the blue flame.

The temperature distribution during the flame spread was measured according to the Thin Filament Pyrometry (TFP) method based on the visible-light radiation from the 14-μm SiC fiber. Since the thermal diffusivity of air is one order greater than that of the SiC fiber, the thermal conduction speed in air is much faster than that in fiber. Therefore, the fiber is heated by hot air during the flame spread. Since the time response of the SiC fiber

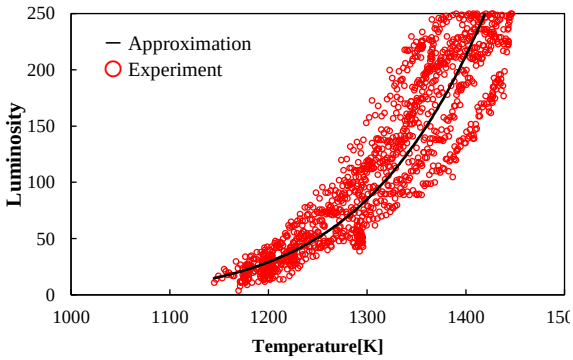

Fig. 6 Relation between temperature and luminosity of R value of RGB image of heated SiC fiber.

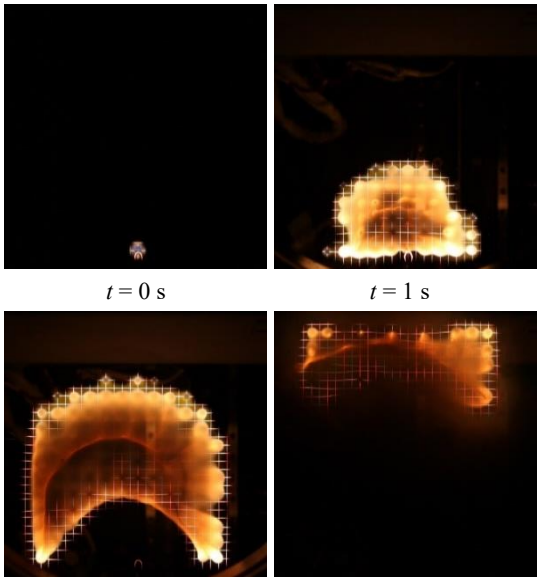

Fig. 7 Sequential images of flame-spread behavior.

to the ambient temperature change is about 1 ms, the temperature of the SiC fiber rapidly follows the gas temperature change[10]. In order to obtain the correlation between the luminance from the SiC fiber and temperature of the SiC fiber, the red value (R value) of the pixel in the RGB image of the SiC fiber heated by a burner was plotted against temperature as shown in **Fig. 6**. The SiC fiber temperature was measured by an R-type thermocouple of 25 μm in wire diameter. The fitting function $R=A\exp(-B/T)$ was used in consideration of the temperature dependence of radiant energy density in Planck's law. T is temperature, A and B are constants. Since this camera does not detect infrared rays, it is effective at 1150 K<T<1450 K in the present TFP method. The temperature error is about ±65 K.

3. Experimental Results and Discussion

The flame-spread behavior of the droplet cloud is shown in **Fig. 7**. The flame spread radially in the early stage. In the later

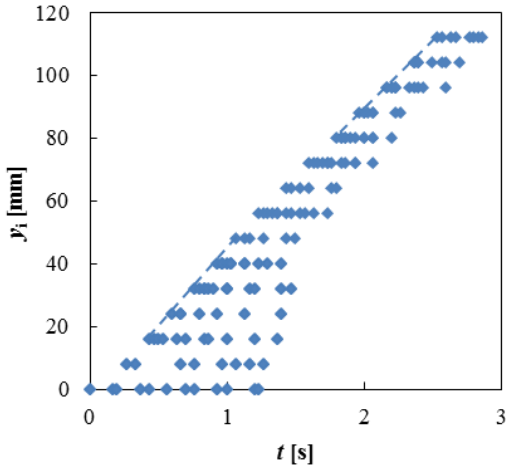

Fig. 8 Temporal variation of droplet ignition position y_i in y-direction.

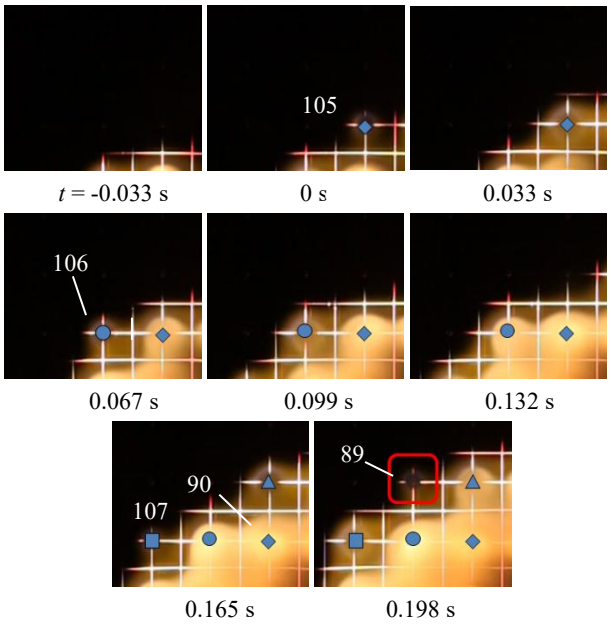

Fig. 9 Sequential photographs of flame spread to Droplet 89.

stage, however, the flame spread mostly in the y-direction. **Figure 8** shows the temporal variation of the droplet ignition position in the y-direction. Since the flame spreads radially after the first ignition, it took longer than 1 s for all droplets located at the small y-position to be ignited. At a large y-position, it took less time for all droplets to be ignited, meaning that the flame spread mostly in one direction. As shown by the dashed lines in **Fig. 8**, the slope of the leading flame position change line became gradual over time. This suggests that the flame-spread rate at the leading flame decreased over time. As shown in **Fig. 4**, since the initial droplet diameter decreased with an increase in the y-position, the relative droplet spacing with respect to the initial droplet diameter increased for a droplet interval of 8 mm and thus the flame-spread rate at the leading flame decreased.

Next, we examined the local flame spread between two adjacent droplets. Unlike the flame spread of droplet arrays, it was difficult to identify the local flame-spread direction of the droplet cloud. Once we had identified the flame-spread direction, we calculated the local flame-spread rate based on each droplet-ignition time of the droplet pair whose connecting direction was closest to the flame-spread direction. This study used three methods of identifying the flame-spread direction; the first method using temperature distributions, the second method considering the luminance distribution of the initial flame right after the ignition and the third method using a comparison of local flame-spread rate candidates with the flame-spread rate of a linear droplet array.

First, we considered temperature distributions during the flame spread. The temperature distribution was approximated from the temperature of the SiC fiber. **Figure 9** shows sequential photographs of flame spread to Droplet 89. **Figure 10** shows the isothermal lines of 1200 K approximated from the 1200 K position on the SiC fiber obtained from **Fig. 9**. Since heat is

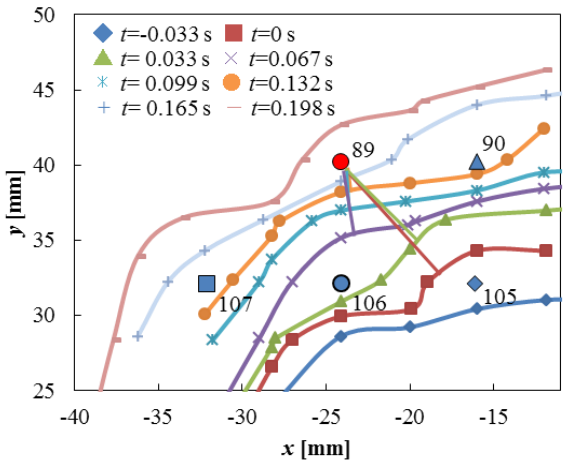

Fig. 10 Temporal variations of isothermal line of 1200 K obtained by TFP method.

conducted perpendicular to the iso-thermal line, we used the perpendicular line from the isothermal line to Droplet 89 each time. From t=0 s to 0.033 s while Droplet 105 was ignited at t=0 s, the heat conducted from Droplet 105 toward Droplet 89. After Droplet 106 was ignited at t= 0.067 s, however, the heat was transferred from Droplet 106 to Droplet 89. At t=0.165 s, Droplet 90 was ignited, and the slight effect of Droplet 90 was observed. The effect of Droplet 106 was still stronger, finally, Droplet 89 was ignited at t=0.198 s. Therefore, the flame spread to Droplet 89 was mainly influenced by the heat transfer from Droplet 106.

Second, we considered the luminance distribution of the initial flame directly after ignition. The left image of **Fig. 11** is a photograph taken when Droplet 89 was ignited. The right image shows the luminance distribution of the red value (R value) of the

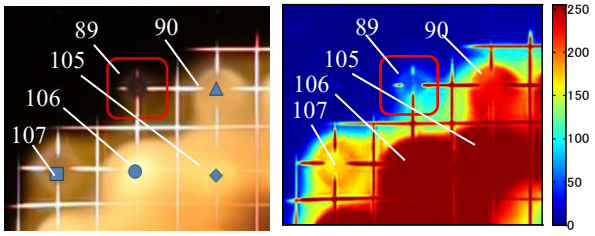

Fig. 11 Luminance distribution of the red value (R value) of RGB image.

RGB image of the left image. Although the initial flame around Droplet 89 partially overlaps the luminance from SiC fibers and another flame, the luminance distribution of the initial flame was not uniform. As discussed by Mikami et al.[1], the ignition process during the flame spread is as follows: an unburned droplet is heated by thermal conduction from a diffusion flame, a flammable mixture layer forms around the droplet, the high-temperature end of the mixture layer is auto-ignited, a triple flame propagates in the mixture layer, and an envelope diffusion flame is established. The color of the diffusion flame changes from blue to yellow due to the soot formation and the yellow luminosity increases over time. Since the high-temperature side of the mixture layer starts burning slightly earlier, the soot also starts forming slightly earlier, resulting in higher luminance in the initial flame. Examining the luminance distribution of the initial flame around Droplet 89, the luminance is lower on the side opposite Droplet 106. Therefore, the combustion in the mixture layer around Droplet 89 probably started from the side of Droplet 106. The flame conceivably spread from Droplet 106 to Droplet 89.

Third, we compared the local flame-spread rate candidates with the flame-spread rate of linear droplet arrays. As shown in **Fig. 9**, Droplets 90, 105, 106 and 107 were already ignited when Droplet 89 was ignited at t=0.198 s. In **Fig. 9**, t=0 s is defined as the moment of the Droplet 105 ignition. Droplet 106 was ignited at t=0.067 s, Droplets 90 and 107 were ignited at t=0.165 s, and Droplet 89 was ignited at t=0.198 s. As shown in **Table 1**, we considered four base-droplet candidates to obtain the local flame-spread rate to Droplet 89. Each local flame-spread rate candidate was calculated from the ignition time difference, the local droplet spacing and the average initial droplet diameter between Droplet 89 and each base-droplet candidate. The droplet spacing between Droplets 90 and 89 was almost the same as that between Droplets 106 and 89. The calculated flame-spread rate for the former is four times as great as that for the latter. The calculated flame-spread rate between Droplets 105 and 89 is close to that between Droplets 106 and 89. However, the droplet spacing for the former is greater than that for the latter. The local flame-spread-rate candidates were compared with the flame-spread rate of linear droplet arrays of Mikami et al.[1]. The calculated flame-spread rate between Droplets 105 and 89 is about three times as great as that of the linear droplet array while the calculated flame-spread rate between Droplets 106 and 89 is about twice as great. Unlike the flame-spread of the linear droplet array, the heat transfer to an unburned droplet must be enhanced by multiple flames in the flame spread in the droplet cloud even though there is a main thermal conduction direction. Therefore, the droplet pair with the minimum increase rate of the local flame-spread-rate candidate with respect to the flame-spread rate of the linear droplet array conceivably shows the main thermal conduction direction, i.e., the main flame-spread direction. **Figure 12** shows the increase rate. The condition with the minimum increase rate is the condition for the base droplet of Droplet 106. This suggests that Droplet 89 was ignited mainly by receiving the thermal influence from Droplet 106. The present three methods give the same flame-spread directions. Thus, the local flame-spread rate to Droplet 89 is $V_f d_0$=47 mm^2/s from Droplet 106.

Table 1 Local flame-spread-rate candidates to Droplet 89 from neighboring Droplets 90, 105, 106 and 107. The flame-spread rate of linear *n*-decane droplet array in microgravity[1] is also listed.

Base droplet No.	S/d_0	Local flame-spread rate $V_f d_0$ [mm^2/s]	Linear droplet array $V_f d_0$ [mm^2/s][1]
90	10.1	1.9×10^2	21.7
105	14.4	44	13.7
106	10.2	47	21.3
107	14.8	2.6×10^2	13.2

The local flame-spread rate is shown in **Fig. 13**. Since there might have been excess heat from the igniter, the local flame-spread rate from the droplet adjacent to the igniter was excluded. **Figure 13** also shows the flame-spread rate of linear *n*-decane-droplet arrays in the microgravity at room temperature and atmospheric pressure by Mikami et al.[1] for comparison. The local flame-spread rate ranges from the same degree as the flame-

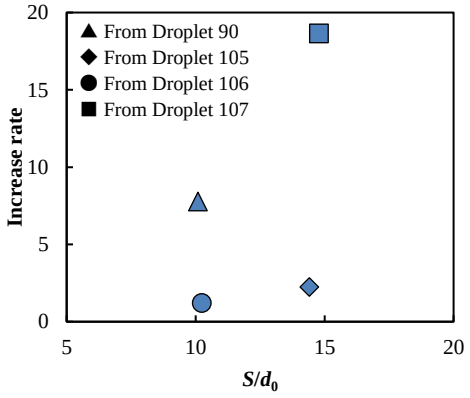

Fig. 12 Increase rate of the local flame-spread rate to Droplet 89 from neighboring droplets in the droplet cloud relative to the flame-spread rate of linear droplet array.

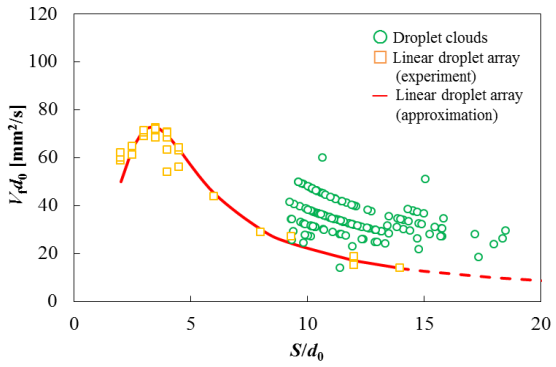

Fig. 13 Dependence of the local flame-spread rate on local droplet spacing. The flame-spread rate of linear *n*-decane-droplet array in microgravity[1] is also plotted.

spread rate of the linear droplet array to nearly three times the rate for the same droplet spacing S/d_0. Mikami et al.[1] reported that the flame-spread-limit droplet spacing $(S/d_0)_{limit}$ is 14 for the linear *n*-decane-droplet array. As shown in **Fig. 13**, there are conditions under which the flame can spread for the local droplet spacing $S/d_0>14$. The increased local flame-spread rate and flame-spread limit was considered to be due to the influence of heat from multiple flames forming a group flame of the droplet cloud. Since the microgravity condition in this experiment was due to a parabolic flight, there was the possibility of a change in gravity during the flame spread. In future, we will further investigate the local flame-spread rate of the droplet cloud by detailed analysis of the results of Group Combustion experiments aboard ISS.

4. Conclusions

As a preliminary experiment of the Group Combustion experiments in the Japanese Experiment Module "Kibo" aboard the International Space Station (ISS), a combustion experiment of unevenly arranged droplet clouds with 148 *n*-decane droplets was conducted in microgravity during parabolic flight of an aircraft. This research proposed three analysis methods to identify the local flame-spread direction. The first method employed the vertical direction from the isothermal line to the unburned droplet. The isothermal line was approximated based on the luminance of SiC fibers tethering droplets. The second method considered the luminance distribution of the initial flame immediately after the ignition. The third method compared the local flame-spread-rate candidates from neighboring droplets with the flame spread-rate of the linear droplet array. It was found that, the local flame-spread direction could be identified by any one of these methods, and the local flame-spread rate was calculated between two droplets close to this direction. The results suggest that there are many conditions under which the local flame-spread rate of an unevenly arranged droplet cloud is greater than the flame spread rate of a linear droplet array. We plan to apply this method to the results analysis of Group Combustion experiments aboard ISS and to analyze the complex flame-spread behavior over randomly-distributed droplet clouds in detail.

References

1) M. Mikami, H. Oyagi, N. Kojima, Y. Wakashima, M. Kikuchi and S. Yoda: Combust. Flame, **146** (2006) 391.
2) H. Oyagi, H. Shigeno, M. Mikami and N. Kojima: Combust. Flame, **156** (2009) 763.
3) H.H. Chiu, H.Y. Kim and E.J. Croke: Proc. Combust. Inst. **19** (1983) 971.
4) M. Mikami, H. Saputro, T. Seo and H. Oyagi: Microgravity Sci. Technol., (2018) in press, DOI: 10.1007/s12217-018-9603-z.
5) M. Mikami, M. Kikuchi, Y. Kan, T. Seo, H. Nomura, Y. Suganuma, O. Moriue and D.L. Dietrich: Int. J. Microgravity Sci. Appl., **33** (2016) 330208.
6) M. Kikuchi, Y. Kan, A. Tazaki, S. Yamamoto, M. Nokura, N. Hanafusa, Y. Hisashi, O. Moriue, H. Nomura and M. Mikami: Trans. JSASS Aerospace Tech. Japan, **12** (2014) No. ists29, Th_25-Th_30.
7) M. Mikami, H. Oyagi, N. Kojima, M. Kikuchi, Y. Wakashima and S. Yoda: Combust. Flame, **141** (2005) 241.
8) T. Farouk and F.L. Dryer: Combustion Theory and Modelling, **15** (2011) 487.
9) H. Nomura, H. Takahashi, Y. Suganuma and M. Kikuchi: Proc. Combust. Inst., **34** (2013) 1593.
10) M. Mikami, H. Watari, T. Hirose, T. Seo, H. Saputro, O. Moriue and M. Kikuchi: J. Thermal Sci. Technol. **12**, (2017) JTST0028.

Acknowledgments

This research was conducted as the "Group Combustion" project by JAXA and was also subsidized by JSPS KAKENHI Grant-in-Aid for Scientific Research (B) (15H04201).